Supporting Information

Modulating Conformation of A*β*-Peptide: an Effective Way to Prevent Protein-Misfolding Disease

Xiang Ma,[†‖] *Jiai Hua,*[‖] *Kun Wang,*[†] *Hongmei Zhang,*[‡] *Changli Zhang,*[§] *Yafeng He,*[†] *Zijian Guo*,*[†] *Xiaoyong Wang*,*[‡]

†State Key Laboratory of Coordination Chemistry, School of Chemistry and Chemical Engineering, Nanjing University, Nanjing 210023, P. R. China. E-mail: zguo@nju.edu.cn; Fax: +86 25 83314502; Tel: +86 25 89684549.

‡State Key Laboratory of Pharmaceutical Biotechnology, School of Life Sciences, Nanjing University, Nanjing 210023, P. R. China. E-mail: boxwxy@nju.edu.cn; Fax: +86 25 83314502; Tel: +86 25 89684549.

‖Chemistry and Chemical Engineering Department, Taiyuan Institute of Technology, Taiyuan, 030008, P. R. China.

§School of Biochemical and Environmental Engineering, Nanjing Xiaozhuang University, Nanjing 210017, P. R. China.

Supplementary Figures and Tables

Table S1 Crystallographic Data and Structural Refinements for CAM

Empirical formula	$C_{32}H_{37}AsCo_4Mo_{12}N_{12}O_{44.50}$
Formula weight	2763.66
Crystal system	Triclinic
Space group	*P*-1
a / Å	11.8532(12)
b / Å	14.5890(13)
c / Å	21.299(2)
α / deg	92.156(2)
β / deg	122.743(6)
γ / deg	109.427(2)
V / Å^3	3393.0(6)
Z	2
D_c / g cm^{-3}	2.705
μ / mm^{-1}	3.674
T / K	293(2)
Limiting indices	$-14 \le h \le 13$
	$-17 \le k \le 16$

	$-25 \le l \le 25$
Measured reflections	17410
Independent reflections	11873
R_{int}	0.0246
Data / restrains / parameters	11873 / 56 / 973
GOF on F^2	1.05
Final R indices [$I > 2\sigma(I)$]	$R_1 = 0.0422$,
	$wR_2 = 0.1059$
R indices (all data)	$R_1 = 0.0655$
	$wR_2 = 0.1134$
Completeness	99.30 %

Table S2 Selected Bond Length (Å) for CAM

Mo(1)-O(1)	1.683(5)	Mo(3)-O(3)	1.673(5)	Mo(5)-O(5)	1.671(5)
Mo(1)-O(14)	1.962(5)	Mo(3)-O(18)	1.983(5)	Mo(5)-O(15)	1.984(6)
Mo(1)-O(17)	1.954(5)	Mo(3)-O(23)	1.996(5)	Mo(5)-O(16)	1.945(5)
Mo(1)-O(26)	2.049(5)	Mo(3)-O(29)	1.817(5)	Mo(5)-O(28)	2.005(5)
Mo(1)-O(27)	2.021(5)	Mo(3)-O(33)	1.859(6)	Mo(5)-O(31)	2.034(5)
Mo(1)-O(37)	2.407(5)	Mo(3)-O(40)	2.459(5)	Mo(5)-O(39)	2.419(5)
Mo(2)-O(2)	1.680(6)	Mo(4)-O(4)	1.690(5)	Mo(6)-O(6)	1.675(5)
Mo(2)-O(14)	1.955(5)	Mo(4)-O(18)	1.984(5)	Mo(6)-O(15)	1.967(5)
Mo(2)-O(17)	1.942(5)	Mo(4)-O(23)	1.995(5)	Mo(6)-O(16)	1.955(5)
Mo(2)-O(29)	2.020(5)	Mo(4)-O(28)	1.854(5)	Mo(6)-O(24)	2.010(5)
Mo(2)-O(34)	2.040(6)	Mo(4)-O(30)	1.820(5)	Mo(6)-O(35)	2.052(6)
Mo(2)-O(40)	2.434(5)	Mo(4)-O(39)	2.482(5)	Mo(6)-O(38)	2.423(5)
Mo(7)-O(7)	1.700(5)	Mo(9)-O(9)	1.672(5)	Mo(11)-O(11)	1.676(6)
Mo(7)-O(19)	1.985(5)	Mo(9)-O(13)	1.977(5)	Mo(11)-O(21)	1.950(5)
Mo(7)-O(20)	1.974(5)	Mo(9)-O(22)	2.013(5)	Mo(11)-O(25)	1.960(5)
Mo(7)-O(24)	1.827(5)	Mo(9)-O(26)	2.042(5)	Mo(11)-O(32)	1.958(5)
Mo(7)-O(32)	1.851(5)	Mo(9)-O(36)	1.955(5)	Mo(11)-O(35)	1.997(6)
Mo(7)-O(38)	2.459(5)	Mo(9)-O(37)	2.414(5)	Mo(11)-O(38)	2.450(5)
Mo(8)-O(8)	1.682(5)	Mo(10)-O(10)	1.678(5)	Mo(12)-O(12)	1.673(6)
Mo(8)-O(19)	2.005(5)	Mo(10)-O(13)	1.961(5)	Mo(12)-O(21)	1.969(6)
Mo(8)-O(20)	2.009(5)	Mo(10)-O(30)	2.019(5)	Mo(12)-O(25)	1.944(5)
Mo(8)-O(22)	1.829(5)	Mo(10)-O(31)	2.023(5)	Mo(12)-O(33)	1.976(5)
Mo(8)-O(27)	1.838(5)	Mo(10)-O(36)	1.954(5)	Mo(12)-O(34)	1.961(5)
Mo(8)-O(37)	2.484(5)	Mo(10)-O(39)	2.429(5)	Mo(12)-O(40)	2.441(5)
Co(1)-O(17)	2.127(7)	Co(2)-O(19)	2.051(5)	Co(4)-O(14)	2.099(5)
Co(1)-O(18)	2.134(5)	Co(2)-N(4)	2.110(7)	Co(4)-O(20)	2.161(5)
Co(1)-O(36)	2.124(5)	Co(2)-N(5)	2.125(7)	Co(4)-O(25)	2.125(5)
Co(1)-N(1)	2.138(7)	Co(3)-O(15)	2.035(6)	Co(4)-N(10)	2.169(8)

Co(1)-N(2)	2.127(7)	Co(3)-O(21)	2.086(6)	Co(4)-N(11)	2.086(8)
Co(1)-O(1W)	2.173(6)	Co(3)-O(23)	2.017(5)	Co(4)-O(2W)	2.195(6)
Co(2)-O(13)	2.035(5)	Co(3)-N(7)	2.097(7)	As(1)-O(37)	1.694(5)
Co(2)-O(16)	2.024(5)	Co(3)-N(8)	2.152(7)	As(1)-O(38)	1.699(5)
As(1)-O(39)	1.691(5)	As(1)-O(40)	1.683(5)		

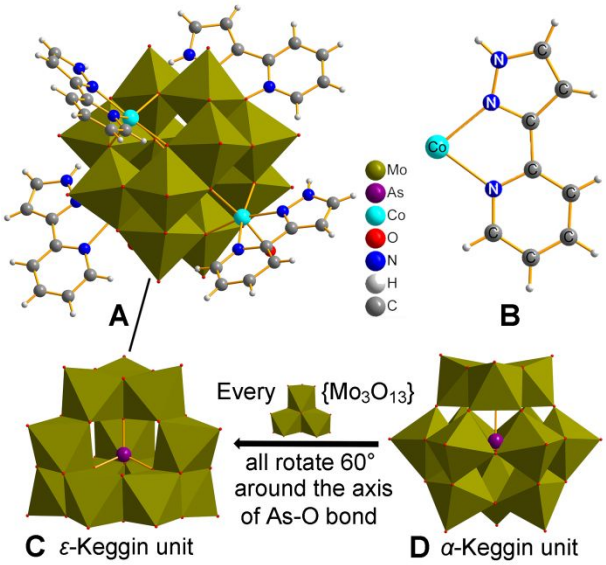

Figure S1. Polyhedral/ball-and-stick representation of CAM (A), $[CoL]^{2+}$ coordination unit (B), ε-$[HAs^{V}Mo^{V}_{6}Mo^{VI}_{6}O_{40}]^{8-}$ monomer (C), and traditional α-Keggin unit (D).

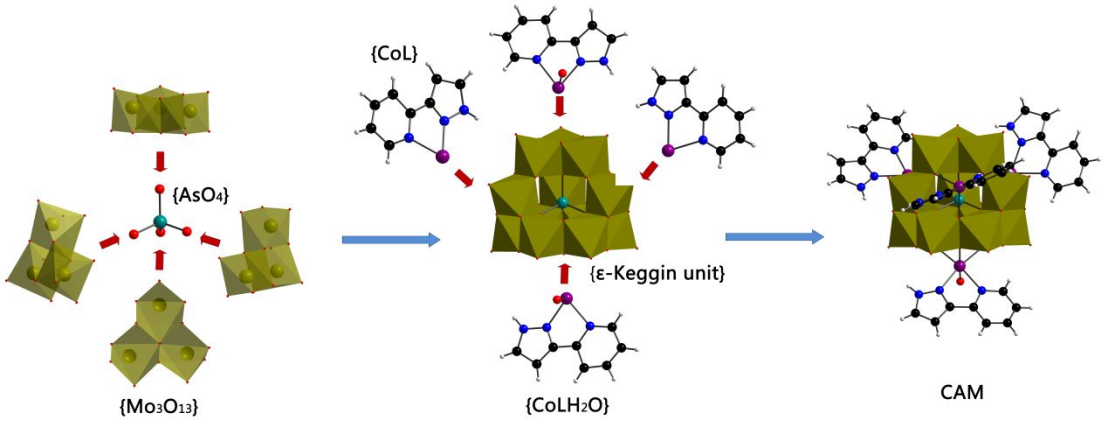

Figure S2. Anatomical diagrams of CAM.

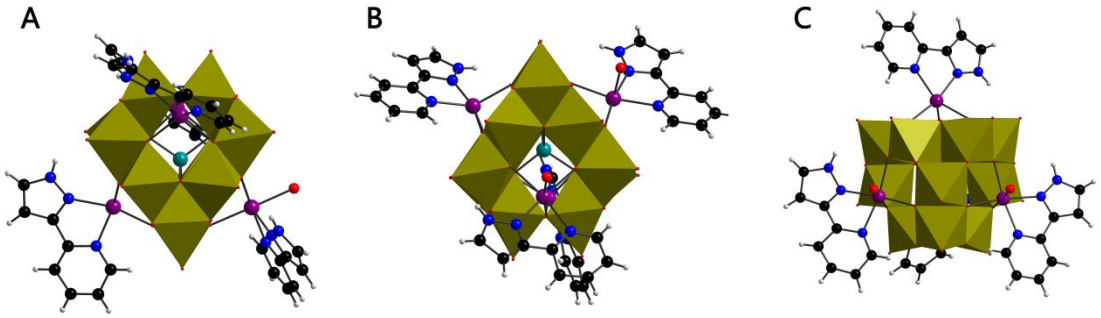

Figure S3. Polyhedral/ball-and-stick representation of CAM via X-axis (A), Y-axis (B), and Z-axis (C).

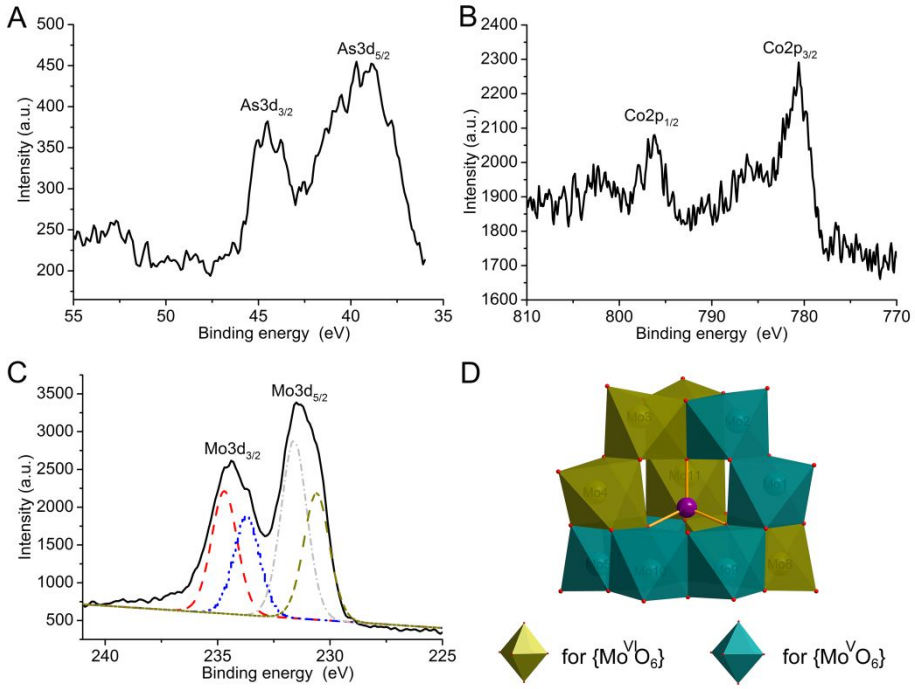

Figure S4. XPS spectra of As, Co and Mo. (A) As^{5+} $3d_{5/2}$ (39.7 eV) and As^{5+} $3d_{3/2}$ (44.5 eV);[1] (B) Co^{2+} $2p_{3/2}$ (780.5 eV) and Co^{2+} $2p_{1/2}$ (796.3 eV);[2] (C) Mo $3d_{5/2}$ (231.4 eV) and Mo $3d_{3/2}$ (234.4 eV). The fitted curves in C (dashed lines) suggest that Mo^{5+} ($3d_{5/2}$, 230.6 eV; $3d_{3/2}$, 233.7 eV) and Mo^{6+} ($3d_{5/2}$, 231.6 eV; $3d_{3/2}$, 234.7 eV) are involved in the peaks of Mo_{3d}.[3] (D) locations of $\{Mo^{V}O_6\}$ and $\{Mo^{VI}O_6\}$ clusters in CAM.

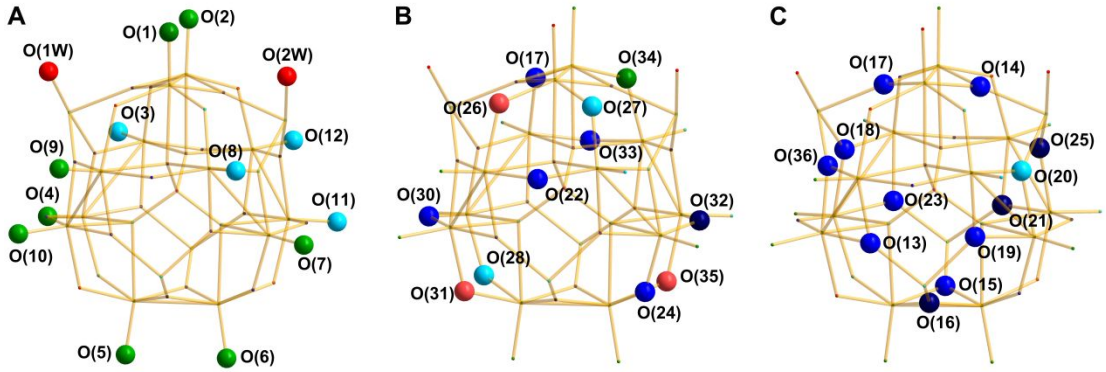

Figure S5. The location and numbering of O_t (A), $O_{\mu 2}$ (B) and $O_{\mu 3}$ (C).

Table S3 Bond Valence Sum (Σs) and Protonation Level (ΣH) of O_t , $O_{\mu 2}$ and $O_{\mu 3}$

Atom	Σs	ΣH	Atom	Σs	ΣH
		O_t			
O(1)	–1.696(1)	0.303(9)	O(8)	–1.834(4)	0.165(6)
O(2)	–1.709(5)	0.290(5)	O(9)	–1.747(3)	0.252(7)
O(3)	–1.879(6)	0.120(4)	O(10)	–1.719(2)	0.280(8)
O(4)	–1.795(2)	0.204(8)	O(11)	–1.863(9)	0.136(1)
O(5)	–1.752(0)	0.248(0)	O(12)	–1.879(1)	0.120(9)
O(6)	–1.733(2)	0.266(8)	O(1W)	–0.272(4)	1.727(6)
O(7)	–1.747(3)	0.252(7)	O(2W)	–0.256(7)	1.743(3)
		$O_{\mu 2}$			
O(17)	–1.968(8)	0.031(2)	O(30)	–1.947(4)	0.052(6)
O(22)	–1.928(2)	0.071(8)	O(31)	–1.333(5)	0.666(5)
O(24)	–1.940(5)	0.059(5)	O(32)	–2.031(8)	–0.031(8)
O(26)	–1.273(5)	0.726(5)	O(33)	–1.965(4)	0.034(6)
O(27)	–1.883(7)	0.116(3)	O(34)	–1.509(1)	0.490(9)
O(28)	–1.862(8)	0.137(2)	O(35)	–1.408(3)	0.591(7)
		$O_{\mu 3}$			
O(13)	–1.962(1)	0.037(9)	O(19)	–1.954(0)	0.046(0)
O(14)	–1.944(0)	0.056(0)	O(20)	–1.872(7)	0.127(3)
O(15)	–1.934(5)	0.065(5)	O(21)	–2.078(1)	–0.078(1)
O(16)	–2.056(3)	–0.056(3)	O(23)	–1.987(8)	0.012(2)
O(17)	–1.968(8)	0.031(2)	O(25)	–2.079(2)	–0.079(2)
O(18)	–1.927(0)	0.073(0)	O(36)	–1.939(7)	0.060(3)

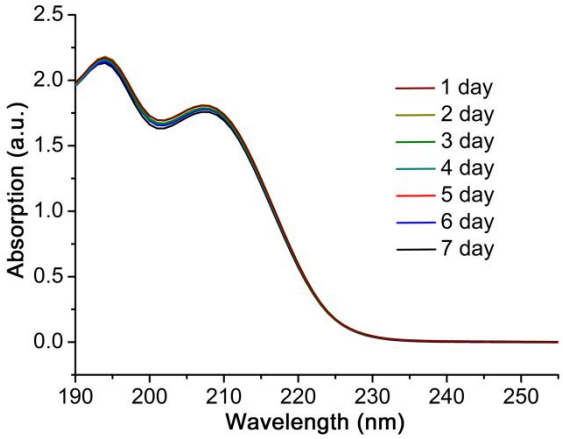

Figure S6. UV-Vis spectra of CAM (10 μM) after incubation in buffer (20 mM Tris-HCl/150 mM NaCl, 5% DMSO, pH 7.4) for 1–7 days.[4] The bands centered at 195 nm are attributed to the pπ→dπ charge transfer transition of the O_t–Mo bonds; the bands at 210 nm are attributed to the pπ→dπ charge transfer transition of the $O_{\mu 2/3}$–Mo bonds.[5]

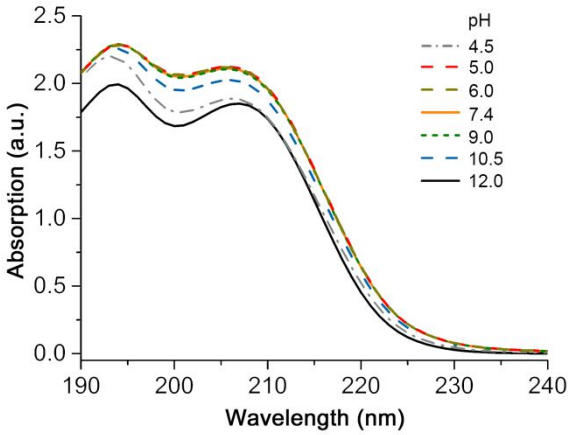

Figure S7. UV-Vis spectra of CAM (10 μM) at different pH values.

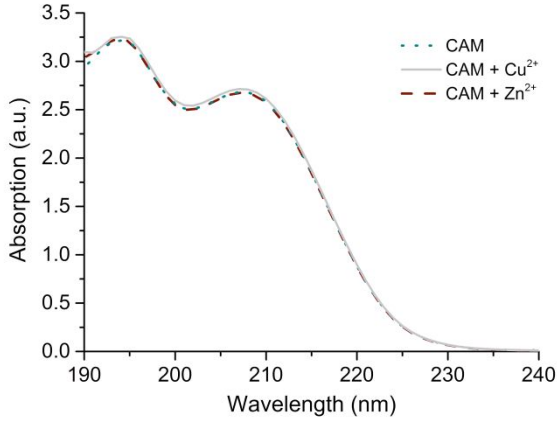

Figure S8. UV-Vis spectra of CAM (20 μM), CAM (20 μM) + Cu^{2+} (20 μM), and CAM (20 μM) + Zn^{2+} (20 μM) after incubation in water solution for 24 h.

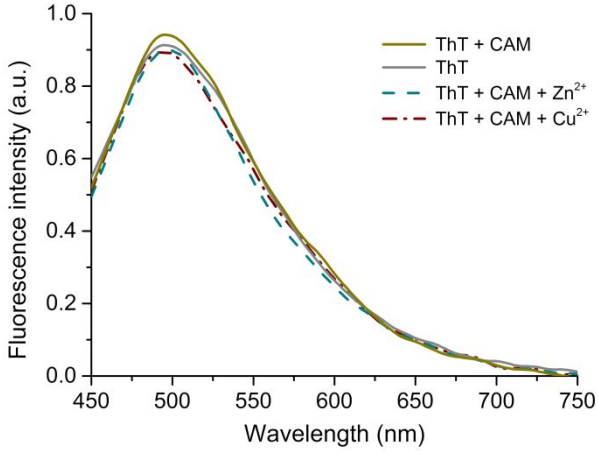

Figure S9. The fluorescence spectra of ThT (30 μM, λ_{ex} = 415 nm) in the absence and presence of Zn^{2+} or Cu^{2+} (20 μM) after incubation with or without CAM (12 μM) in aqueous solution at 37 ºC and pH 7.4 for 24 h.

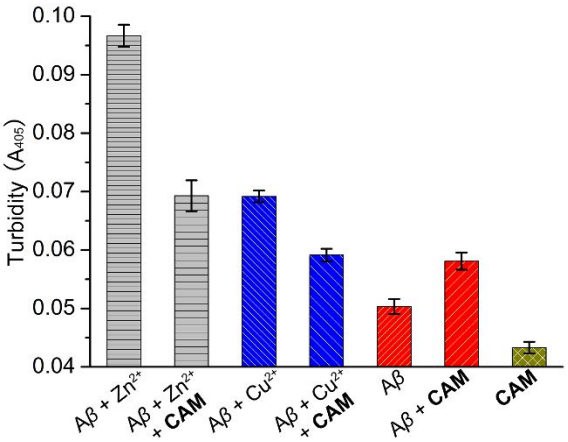

Figure S10. Turbidity (A_{405}) of Aβ40 solutions (20 μM) after incubation with or without Zn^{2+} or Cu^{2+} in the absence and presence of CAM at 37 ºC and pH 7.4 for 24 h ([Aβ40] : [metal ion] : [CAM] = 1 : 2 : 0.6).

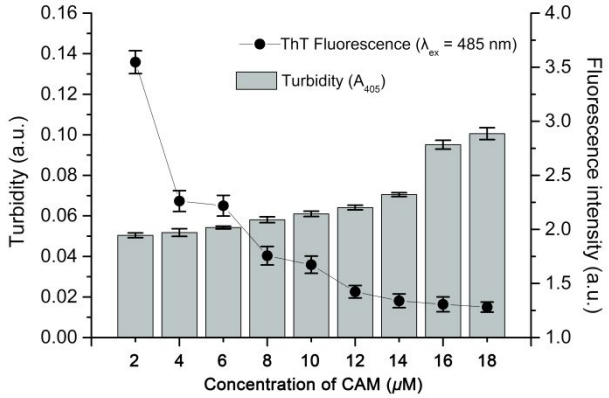

Figure S11. The effect of CAM on the Aβ40 (20 μM) aggregates determined by ThT assay (λ_{ex} = 415 nm, λ_{em} = 480 nm) and the corresponding turbidity.

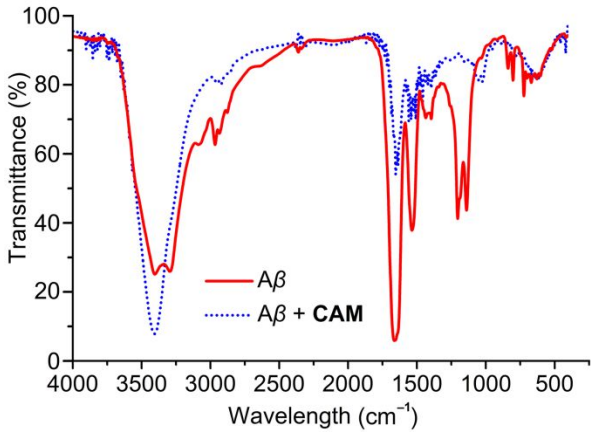

Figure S12. IR spectra for Aβ40 and Aβ40 incubated with CAM at 37 ºC.

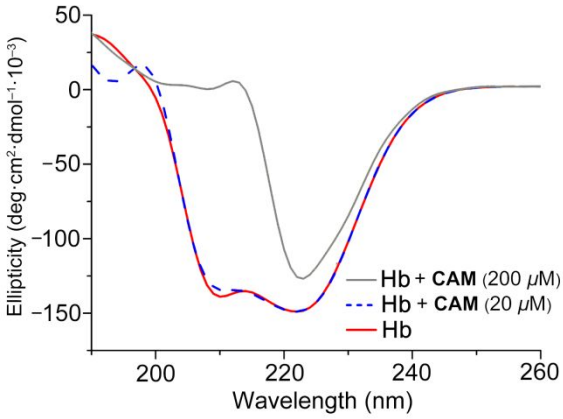

Figure S13. CD spectra of Hb (20 μM) with or without CAM (20 and 200 μM) after incubation at 37 °C.

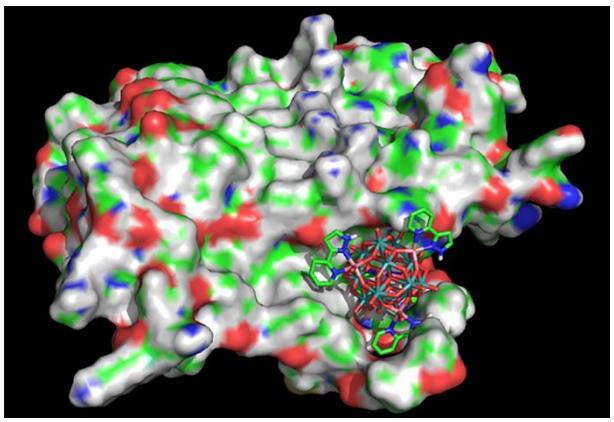

Figure S14. Detailed surroundings of the CAM-Aβ complex.

References

[1] Yang, D.; Liang, Y.; Ma, P.; Li, S.; Wang, J.; Niu, J. Ligand-directed conformation of inorganic–organic molecular capsule and cage. *Inorg. Chem.* **2014**, *53*, 3048–3053.

[2] Melaet, G.; Ralston, W. T.; Li, C. S.; Alayoglu, S.; An, K.; Musselwhite, N.; Kalkan, B.; Somorjai, G. A. Evidence of highly active cobalt oxide catalyst for the Fischer–Tropsch synthesis and CO_2 hydrogenation. *J. Am. Chem. Soc.* **2014**, *136*, 2260–2263.

[3] Zhang, Y. P.; Li, L. L.; Sun, T.; Liu, B.; Hu, H. M.; Xue, G. L. A Cagelike polyanion with a Ag^+ enwrapped, $[AgAs_2Mo_{15}O_{54}]^{11-}$. *Inorg. Chem.* **2011**, *50*, 2613–2618.

[4] Gao, N.; Sun, H. J.; Dong, K.; Ren, J. S.; Duan, T. C.; Xu, C.; Qu, X. G. Transition-metal-substituted polyoxometalate derivatives as functional anti-amyloid agents for Alzheimer's disease. *Nat. Commun*. **2014**, *5*, 3422–3431.

[5] Niu, J.; Hua, J.; Ma, X.; Wang, J. Temperature-controlled assembly of a series of inorganic–organic hybrid arsenomolybdates. *Crystengcomm* **2012**, 14, 4060–4067.